First-principles study of valence and structural transitions in EuO under pressure

L. Petit,[1] Z. Szotek,[1] M. Lüders,[1] W. M. Temmerman,[1,†] and A. Svane[2]
[1]*Daresbury Laboratory, Warrington WA4 4AD, United Kingdom*
[2]*Department of Physics and Astronomy, Aarhus University, DK-8000 Aarhus C, Denmark*
(Received 24 September 2013; revised manuscript received 20 May 2014; published 10 July 2014)

The electronic structure of EuO under pressure is studied using the self-interaction corrected local spin density approximation. EuO, which at ambient conditions crystallizes in the NaCl (B1) structure, is predicted to undergo an isostructural insulator to metal transition at 48 GPa. This transition is associated with a change of valence from a divalent to an intermediate valent state, with the resulting effective valency of 2.35. The pressure range between 48 and 70 GPa is characterized by the competition between an intermediate valent B1 structured phase and a CsCl (B2) structured phase where both the divalent and intermediate valence configurations are in play. Eventually, at pressures above 70 GPa, the intermediate valent B2 phase prevails. The effective Eu valence in the B2 intermediate valence phase is around 2.28, i.e., a decrease in effective valence occurs. This scenario is in line with the reentrant valence behavior observed in recent pressure experiments.

DOI: 10.1103/PhysRevB.90.035110 PACS number(s): 71.15.Nc, 71.27.+a, 71.30.+h, 71.23.An

I. INTRODUCTION

The rare earth monochalcogenides exhibit a remarkable variety in electronic properties, driven by a complex interplay of ligand chemistry and dual character of f electrons that determine the underlying valency [1]. Of particular interest are compounds situated at the boundary of an f-electron localization-delocalization transition, where a change in valency is brought about by changes in the external parameters, such as pressure, temperature, or alloying. A well known example is SmS, which at low temperature and zero pressure crystallizes in the NaCl structure with semiconducting behavior (black color phase), and which at a moderate pressure of 0.65 GPa turns metallic (golden color phase), with an associated significant volume collapse of 13.5% [2]. Features such as the occurrence of an isostructural phase transition upon compression, or an anomalous pV curve, are distinct signatures of valence transformations. Apart from the Sm chalcogenides [2], valence transitions under pressure have been observed in Eu [3], Tm [4], and Yb [5] chalcogenides. In the present study the focus is on EuO, where the combination of valence instabilities with the fact that this is one of only a very few ferromagnetic semiconductors [6] known to exist holds great potential for device applications.

Photoemission studies [7] on EuO reveal an electronic structure characterized by the localized Eu-f states situated in the semiconducting gap separating the O-2p valence band from the Eu-5sd conduction band. At ambient temperature, the observed optical absorption edge places the occupied f level at around 1.0 eV below the unoccupied d states. From optical absorption measurements at 20 K [8], it was established that EuO remains semiconducting below the Curie temperature, although the shift of the absorption edge to lower energies indicates an energy gap that is reduced by roughly 0.3 eV. The redshift was subsequently explained by the onset of exchange interactions below T_C that split the conduction band spin-up and spin-down states, resulting in a reduced energy gap between the f states and the conduction band [9], also confirmed by recent spin-resolved x-ray absorption measurements [10].

A series of experiments over the years have resulted in a somewhat unclear picture concerning the valence instabilities in EuO under pressure. In an early study, Jayaraman observed an isostructural semiconductor to metal transition at around 30 GPa [11]. The associated volume collapse of about 4% was ascribed to a change in the valence state of Eu from divalent to trivalent. A further abrupt volume collapse observed at around 40 GPa was associated with the NaCl to CsCl structural transition. Zimmer *et al.* [12] confirmed the observed insulator to metal transition in EuO under pressure, commencing however at a much lower pressure of 13 GPa, and from the absence of any noticeable volume collapse up to 37 GPa, they concluded that EuO undergoes a continuous valence transition. On the other hand, Mössbauer measurements on EuO under pressure up to 31 GPa did not find indications of a noticeable valence change at all [13]. This latter observation agrees with an x-ray diffraction study by Heathman *et al.* where no valence transition was observed up to 47 GPa, at which point a structural NaCl→CsCl transition sets in that is not quite complete at 63 GPa [14]. Finally, a recent study, using x-ray absorption near edge structure (XANES) [15], seems to largely confirm the measurements by Jayaraman *et al.*, with an isostructural valency transition observed around 35 GPa accompanied by a modest 0.5% volume collapse, and beginning around 45 GPa a structural transition to the CsCl structure, which is fully completed around 60–65 GPa.

With respect to the theoretical studies, the local spin density (LSD) approximation to exchange and correlation fails to correctly describe the electronic structure of strongly correlated electron systems and the Eu chalcogenides, with their localized 4f states, are no exception to this rule. Applying the LSD based band picture to the 4f electrons results in narrow f bands situated at the Fermi level, predicting EuO to be metallic [16]. In early calculations based on the Slater

[†]Deceased 10 May 2014.

exchange potential, Cho [17] showed that a reduced exchange potential gave rise to the correct energy gaps and relative f-band positions. However, the more recent calculations all use approximations that go beyond LSD when trying to address the correlated nature of the f electrons. Methods based on hybrid functionals use an admixture of local (or semilocal) exchange-correlation functional with nonlocal Hartree-Fock [18]. In LDA+U [16,19] and LDA+DMFT [20] calculations the Hubbard U parameter is introduced to account for the effect of strong correlations. Given a reasonable value for the U parameter, methodologies such as LDA+U [16,19], DMFT [20], or QSGW+U [21], are able to accurately reproduce the spectroscopic features of EuO at ambient pressure. Also, assuming U to remain constant under pressure has been shown to be an acceptable approximation when analyzing changes in magnetic ordering [20,22]. In general, however, there is no well defined and/or justified approach to describing changes of U under pressure, therefore an insulator (large U) to metal ($U \sim 0$) transition cannot be adequately represented.

The self-interaction corrected (SIC)-LSD method, applied here for studying valence instabilities and structural transitions of EuO under pressure, requires no additional parameters and distinguishes between localized (insulator) and delocalized (metal) f-electron states, based on total energy considerations. This approach is briefly described in the next section, while the results and discussion of our calculations are presented in Sec. III. Our conclusions are summarized in Sec. IV.

II. SIC-LSD

The SIC-LSD method is designed to correct the LSD approximation for the unphysical interaction of an electron with itself [23–25]. The latter can become quite significant for a localized electron, although it all but vanishes for an itinerant band state [26]. SIC-LSD addresses this problem by associating a gain in energy with electron localization. The corresponding, orbital dependent, total energy functional describes a manifold of coexisting localized and delocalized electrons. For delocalized states the SIC energy vanishes and the electron behaves as an extended state described within LSD, with the corresponding gain in band formation energy. The localized state loses this band formation energy, but instead is constrained to remain on-site by the attractive SIC potential, which results in a corresponding gain in SIC energy determining whether a given f electron prefers to localize or remain itinerant. Different localized/delocalized configurations are realized by assuming different numbers and combinations of localized states (here f states on the rare earth atom). Since the different localization scenarios constitute distinct local minima of the same energy functional, their total energies may be compared and the global energy minimum then defines the ground-state total energy and the nominal valence configuration of the rare earth ion.

Here the nominal valence is defined as an integer number of electrons available for band formation, namely $N_{\mathrm{val}} = Z - N_{\mathrm{core}} - N_{\mathrm{SIC}}$, where Z is the atomic number, N_{core} is the number of core (and semicore) electrons, and N_{SIC} is the number of localized, i.e., self-interaction corrected, electron states. In the case of EuO, for the Eu atom $Z = 63$, the number of core electrons N_{core} is 54, and the number of self-interaction corrected, localized, f electrons can be maximum seven, in which case Eu would be in a divalent 2+ state. For a trivalent Eu, only six f electrons are considered as localized, and thus self-interaction corrected, while the seventh f electron is allowed to partially or fully delocalize and through hybridization with the spd electrons contribute to bonding, and to the resulting valence. Although the nominally divalent and trivalent Eu states differ by one, in terms of charge they only differ by a fraction of an f electron, and thus represent an effective, or intermediate, valence of between 2.0 and 3.0. The nominally trivalent state could only be realized if the seventh f electron got fully delocalized and promoted to the spd valence band. As opposed to the intermediate valency, a mixed valence system would be obtained if there was a mixture of divalent and trivalent Eu ions in a pseudoalloy sense [27]. For completeness note that in the standard definition, the valency is defined as an integer number of electrons in the outermost shell of an atom.

III. RESULTS AND DISCUSSION

In this section we present results and discussion of the SIC-LSD calculations for EuO under pressure. The key properties comprise total energies, enthalpies, valences, transition pressures, and electronic structure, for both the NaCl(B1) and CsCl(B2) structures. By studying the relevant valence (oxidation) states of Eu in both structures under pressure we aim to shed more light on the resulting valence and structural transitions, and the respective transition pressures, in close relation to the experimental evidence.

A. Total energy, enthalpy, and transition pressures

In Fig. 1 the SIC-LSD total energies, calculated for EuO in both the NaCl (B1) and CsCl (B2) structures, are displayed as functions of volume. For each structure the two energetically

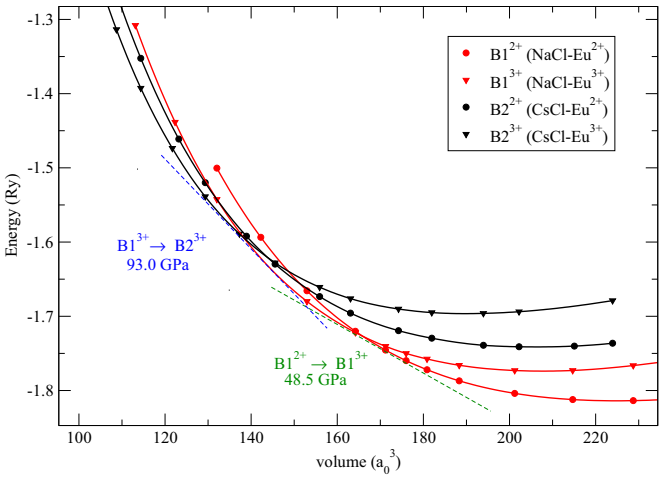

FIG. 1. (Color online) Total energy of EuO under pressure. The red and black colors highlight the NaCl (B1) and CsCl (B2) structures, respectively. $B1^{2+}$ and $B2^{2+}$ refer to the $Eu^{2+}(f^7)$ configuration. $B1^{3+}$ and $B2^{3+}$ refer to the $Eu^{3+}(f^6)$ configuration. The dashed lines represent the common tangents for the $B1^{2+} \rightarrow B1^{3+}$ valence transition (dark green) and the $B1^{3+} \rightarrow B2^{3+}$ structural transition (blue), respectively.

relevant configurations shown are the divalent $Eu^{2+}(f^7)$ and trivalent $Eu^{3+}(f^6)$ oxidation states. They respectively correspond to seven and six localized f electrons per Eu site. Configurations representing higher valence states, such as $Eu^{4+}(f^5)$, $Eu^{5+}(f^4)$, etc., are found to be energetically unfavorable and are not shown here. In agreement with experiment, the calculated global energy minimum is obtained in the insulating state with a divalent $Eu^{2+}(f^7)$ configuration and the B1 structure ($B1^{2+}$). The corresponding equilibrium volume is equal to 225 a_0^3 (the experimentally observed volume equals to 228 a_0^3) [28]. With increasing pressure, i.e., in Fig. 1 when moving towards smaller volumes with respect to the equilibrium volume, we observe the trivalent Eu configuration ($B1^{3+}$) gradually becoming energetically more favorable and, at compressed volume of around 170 a_0^3, the latter eventually becomes the ground state, indicating an isostructural (NaCl), delocalization transition, from $Eu^{2+}(f^7)$ to $Eu^{3+}(f^6)$. The corresponding transition pressure, defined by the slope of the common tangent (dashed green line), is evaluated to be 48.5 GPa. Increasing the pressure even further, at a volume of around 145 a_0^3, the CsCl structure becomes energetically more favorable. This structural transition, from $B1^{3+} \rightarrow B2^{3+}$, occurs at a pressure of 93 GPa (the common tangent indicated by dashed blue line), and is characterized by a slight reduction in effective valency, although the nominal valence remains unchanged (3+).

The calculations confirm the occurrence of an isostructural valency transition in the B1 phase, although the predicted transition pressure (48.5 GPa) is somewhat higher than the experimentally observed values (ranging from 30 to 37 GPa) [11,12,15]. However, our predicted $B1^{3+} \rightarrow B2^{3+}$ transition above 90 GPa clearly overestimates the experimentally observed structural transition, seen to be completed at around 65–70 GPa (setting in around 45 GPa) [12,15]. A possible reason for overestimating the structural transition pressure is that in the present work, the electron wave functions are expanded in terms of the linear muffin-tin orbital (LMTO) basis functions [29], within the atomic spheres approximation (ASA), whereby the crystal volume is divided into slightly overlapping atom centered spheres of a total volume equal to the actual volume. A well known shortcoming of ASA is that different crystal structures have different degrees of overlap of the ASA spheres, resulting in substantial relative errors in the evaluation of the total energy. While this inhibits the comparison of energies of different crystal structures, when comparing the energies of different localization scenarios [here $Eu^{2+}(f^7)$ to $Eu^{3+}(f^6)$] within the same crystal structure the ASA error is of minor influence.

To correct for the relative total energy error between the B1 and B2 structures, we use the experimentally observed transition pressure to calibrate the total energy curves, by shifting them with respect to each other until the slope of the resulting common tangent gives the transition pressure equal to the experimentally observed value [30]. Thus substituting the experimentally observed structural transition pressure (60 GPa) for the calculated one (93 GPa) implies changing the slope of the corresponding common tangent, giving rise to a rigid shift of 18 mRy per formula unit for the B2 total energy curves relative to the B1 curves, as demonstrated in Fig. 2. Here the region around the structural transition is magnified

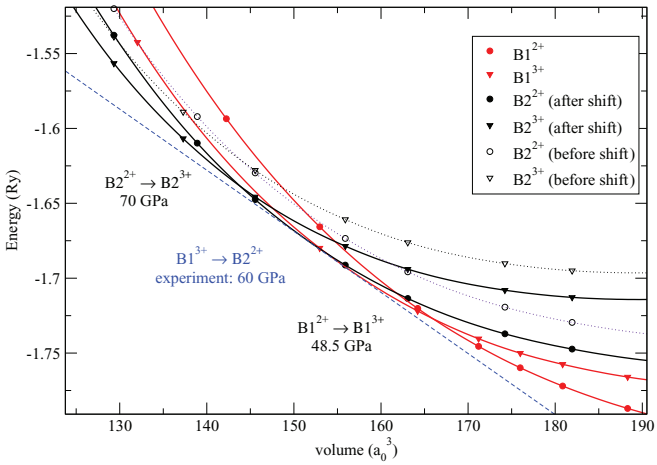

FIG. 2. (Color online) Total energy of EuO as a function of volume. The red and black colors highlight the NaCl (B1) and CsCl (B2) structures, respectively. $B1^{2+}$ and $B2^{2+}$ refer to the $Eu^{2+}(f^7)$ configuration. $B1^{3+}$ and $B2^{3+}$ refer to the $Eu^{3+}(f^6)$ configuration. The black dotted lines refer to the original B2 total energy curves, while the black solid lines present the same curves, but shifted vertically down by 18 mRy (see text for discussion) until they touch the common tangent line representing the experimentally observed structural transition pressure (blue dashed line).

for clarity. The original total energy curves (Fig. 1) for the B2 structure are indicated by the dotted black lines, while the shifted total energy curves are given by the solid black lines. The slope of the common tangent (blue dashed line) is set by the experimentally observed B1 to B2 transition pressure.

As one can observe from Fig. 2, due to the shift of the B2 curves relative to the B1 curves, the overall picture changes. Most noticeably the structural transition (now at the experimentally determined value of 60 GPa) is no longer isovalent from $B1^{3+}$ to $B2^{3+}$, but instead reentrant from $B1^{3+}$ to $B2^{2+}$, i.e., with an associated decrease in valency. As a consequence EuO under pressure is characterized by a sequence of three transitions, respectively, an isostructural valence transitions in the B1 phase at 49 GPa, a stuctural reentrant transition around 60 GPa, and a further isostructural valence transition now in the B2 phase at 70 GPa. With the B2 curves overall having moved closer energetically to the B1 curves, even before the full-fledged structural transition takes place, beginning with volumes around 163 a_0^3, the $B1^{3+}$ and $B2^{2+}$ configurations are close to degenerate in energy, indicating competition between NaCl and CsCl phases. This is more clearly illustrated in Fig. 3(a), where the enthalpies of the B1 and B2 structures, each with both the 2+ and 3+ Eu configurations, are shown as functions of pressure. Below 40 GPa, the $B1^{2+}$ phase has significantly lower enthalpy than any of the other phases, while above 80 GPa the $B2^{3+}$ has distinctly the lowest enthalpy. In the pressure range between ~40 and ~80 GPa, the lowest enthalpy phase changes with increasing pressure as $B1^{2+}$, $B1^{3+}$, $B2^{2+}$, and $B1^{3+}$. Also one notices that in this pressure range, always two or even three phases have similar enthalpies within 5 mRy, and we speculate that experimentally this situation will lead to a system of mixed crystal structures and mixed valencies for pressures

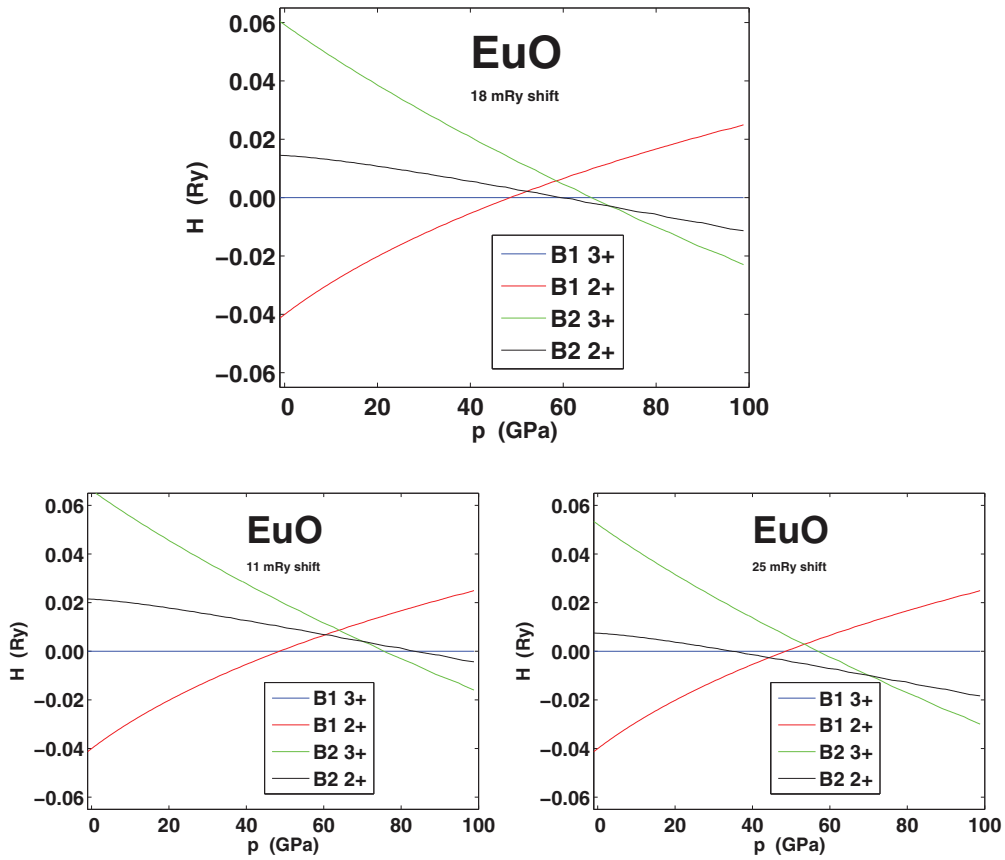

FIG. 3. (Color online) EuO under pressure. Enthalpy as a function of pressure for the different phases of EuO relative to that of the $B1^{3+}$ phase (blue). The $B1^{2+}$ is shown in red, the $B2^{2+}$ in black, and the $B2^{3+}$ in green. (a) Corresponds to Fig. 2 with an assumed structural transition of 60 GPa requiring an 18 mRy ASA related energy shift of the B2 phase relative to the B1 phase. (b) and (c) represent alternative scenarios, assuming, respectively, an ASA energy correction of 11 and 25 mRy, corresponding to transition to the B2 structure at pressures of 75 and 45 GPa.

between ∼40 and ∼80 GPa, with high sensitivity of actual proportions of the various phases to strain and/or temperature inhomogeneities as well as sample imperfections.

In their pressure experiments Souza-Neto *et al.* [15] observe a coexistence of trivalent (Eu^{3+}) NaCl and divalent (Eu^{2+}) CsCl structures in the range between 44 and 60 GPa, and a complete transition to the divalent CsCl structure above 60 GPa, which altogether is in good agreement with the present theoretical picture. Our analysis is of course somewhat empirical, since the 18 mRy ASA-correction energy shift that was applied in Figs. 2 and 3(a) has been derived from equalizing the calculated structural transition pressure with the experimentally observed value. Here we used 60 GPa, referring to the pressure where the structural transition from NaCl to CsCl is complete. Assuming for example structural transition pressures above 75 GPa or below 45 GPa results in the enthalpy versus pressure behavior depicted, respectively, in Figs. 3(b) and 3(c). The decrease/increase in transition pressure results in an decreased/increased common tangent, and is reflected by an increase/decrease in the ASA-related correction energy. The differences to the 60 GPa scenario are noticeable, with Fig. 3(c) ($P \sim 45$ GPa) revealing a $B1^{2+} \rightarrow B2^{2+}$ structural transition without prior valence transition, and Fig. 3(b) ($P \sim 75$ GPa) depicting an isovalent $B1^{3+} \rightarrow B2^{3+}$ structural transition quite similar to Fig. 1. However, the scenarios displayed in Figs. 3(b) and 3(c) are somewhat extreme, and for transition pressures in the experimentally observed range ∼50 to ∼65 GPa, the scenario will be qualitatively as in Fig. 3(a) albeit with some quantitative deviations.

In a full potential implementation the problems associated with ASA do not occur, as all the nonspherical contributions to the potential are included, and no shape approximation to the crystal geometry is invoked. Unfortunately SIC-LSD has as yet not been implemented in a full potential version. In this work we have selected the atomic sphere radii based on the criterion that the Coulomb potential—evaluated for overlapping neutral atoms placed in the crystal structure at the experimental lattice constant—be minimal at the separation point for nearest neighbors. This gives atomic sphere radii $R(\mathrm{Eu}) = 3.34\, a_0$ and $R(\mathrm{O}) = 2.23\, a_0$ at the experimental equilibrium volume in the B1 phase. [For the B2 phase which only exists under pressure, we use the values $R(\mathrm{Eu}) = 3.30\ a_0$ and $R(\mathrm{O}) = 2.41\ a_0$ as obtained instead at the theoretical equilibrium volume.] The ratios of atomic radii are subsequently kept unchanged during variation of the crystal volume. The relative error introduced by the ASA can be estimated from a comparison of the total energies as obtained, respectively, with a full-potential method [31] and the ASA calculation, when both are applied to the f^0 (LSD) configuration. The corresponding calculation for EuO finds that a 14 mRy energy shift of the B2 total energy

curve, relative to the B1 total energy curve, is required to align the ASA and FP minima, in rather good agreement with the 18 mRy required to align the calculated ASA transition pressure with experiment in Fig. 3(a).

B. Electronic structure

The SIC-LSD calculations predict the ground state of EuO at zero pressure to be divalent, $Eu^{2+}(f^7)$, with seven localized f electrons resulting in electronic structure characterized by an insulating gap between O-p states and Eu-d states of 2.40 eV. It is important to notice that the focus of the SIC-LSD approach is on total energies. It is after all a one-electron ground state theory, which does not give accurate removal energies of localized states due to electron-electron interaction (multiplet) effects [32] and the neglect of screening and relaxation effects [33]. In the case of EuO these occupied f states appear as sharp resonances unrealistically far below the conduction band minimum. A rough estimate of the removal energies may be obtained by the transition state argument [34], which places the f peak midway between its calculated SIC-LSD and LSD positions, which however does not effect the total energies, or their variation under pressure.

Here we concentrate on the changes in the electronic structure of EuO that occur during the structural transition, using the calculated densities of states (DOS) for the B1 and B2 structures in the trivalent configuration. Both DOS curves, respectively, in Fig. 4(a) for $B1^{3+}$ and in Fig. 4(b) for $B2^{3+}$, have been calculated at a volume of 156 a_0^3, where, as can be seen from the total energy plot in Fig. 2, the Eu^{3+} configuration is the energetically most favorable configuration in the B1 structure, but energetically unfavorable, compared to the Eu^{2+} configuration, in the B2 structure. Overall, we observe the O-p band separated by a gap from the Eu-d states, and most noticeably a large narrow f peak, pinning the Fermi level, and resulting from the fact that in the trivalent configuration one of the majority f states is treated as a delocalized band state. The remaining six majority f states continue to be treated as localized, and are not shown in the DOS plots, as they are situated at lower energies. The minority f states occur above the Fermi level, separated from the majority f peak by the exchange splitting. The large moment on the Eu ions results in the splitting between spin-up and spin-down d states at the bottom of the conduction band. This is also observed in the divalent configuration at the equilibrium volume, where the exchange splitting at the bottom of the conduction band is found to be 0.57 eV, in good agreement with the experimental value of 0.60 eV [10].

From the SIC-LSD perspective, filling the narrow f peaks results in a marginal gain in binding energy, and the gain in SIC energy associated with the localization of the corresponding f state is relatively larger. Consequently, the almost fully occupied f peak makes the trivalent configuration shown in Fig. 4(b) energetically unfavorable, and at volumes around 156 a_0^3, in the CsCl phase, the divalent configuration is energetically more favorable, as can also be seen in Fig. 2. In the trivalent NaCl phase, depicted in Fig. 4(a), the peak is rather less occupied, indicating that more electrons have transferred to d states. For a given volume, the Eu-O distance is smaller in the B1 structure compared to the B2 structure.

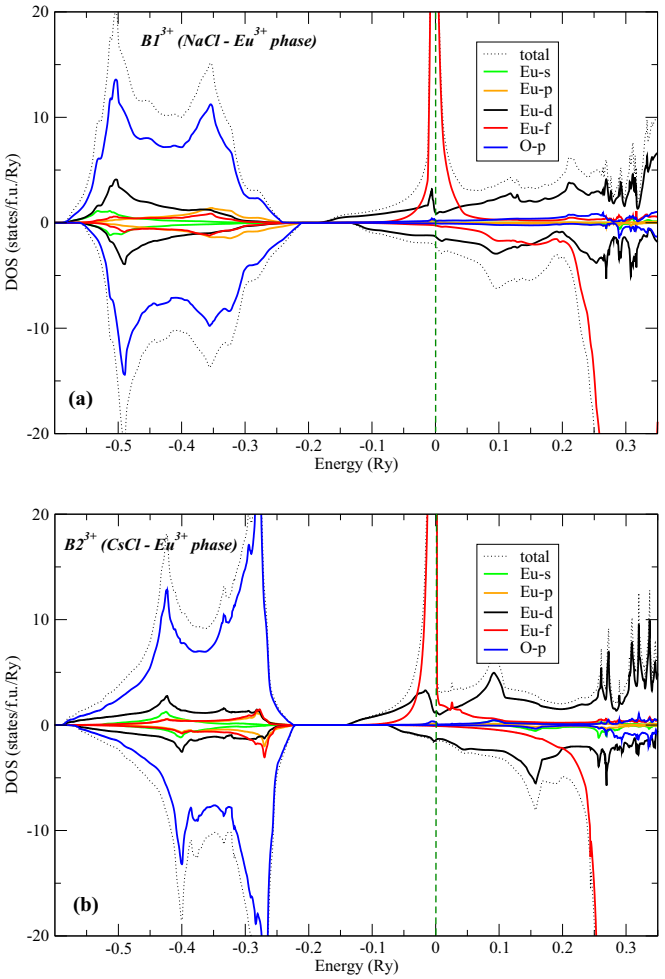

FIG. 4. (Color online) Density of states (in states/formula unit/Ry) for EuO in the trivalent Eu configuration at a volume of 156 a_0^3. (a) NaCl structure and (b) CsCl structure. The positive and negative DOS refer to up and down spin states, respectively. The total DOS is indicated by the black dotted lines, the site decomposed DOS are indicated by the colored solid lines. Energy is in Ry, and the Fermi level is situated at zero energy.

This results in larger overlap between the O-p and Eu-d states in the B1 structure, and therefore, broader energy bands and a reduced band gap (0.34 eV compared to 1.06 eV in the B2 structure). Due to the increased overlap, the d states are situated at lower energy with respect to the f peak and accommodate additional electrons, leaving the f states partially unoccupied. Compared to filling the narrow f peak, the gain in binding energy associated with filling the broad d states is rather large, overcoming the gain in SIC energy, associated with a possible localization of the f state, and consequently, in the NaCl phase, at around 156 a_0^3, the trivalent configuration depicted in Fig. 4(a) is energetically most favorable.

C. Valence and f-electron character

The dual character of f electrons, localized vs itinerant, and its relevance for valence of an element, was discussed in many earlier papers (e.g., [35–37]). Here we study the effective valence of EuO under pressure for both the B1 and

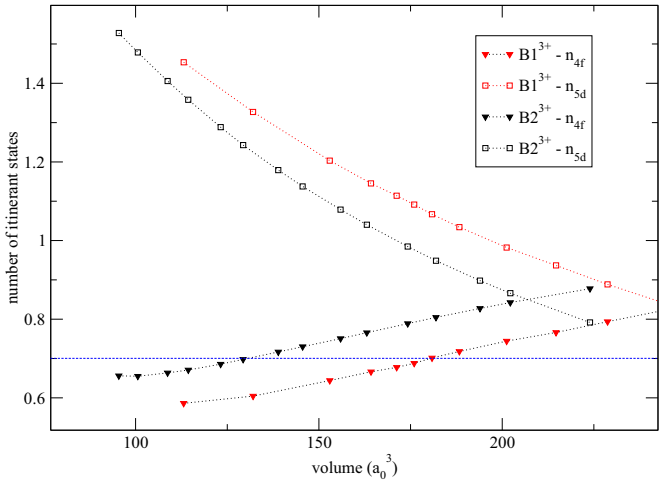

FIG. 5. (Color online) Number of delocalized $4f$ and $5d$ electrons as a function of volume in EuO for both the NaCl and the CsCl structures in the trivalent configuration.

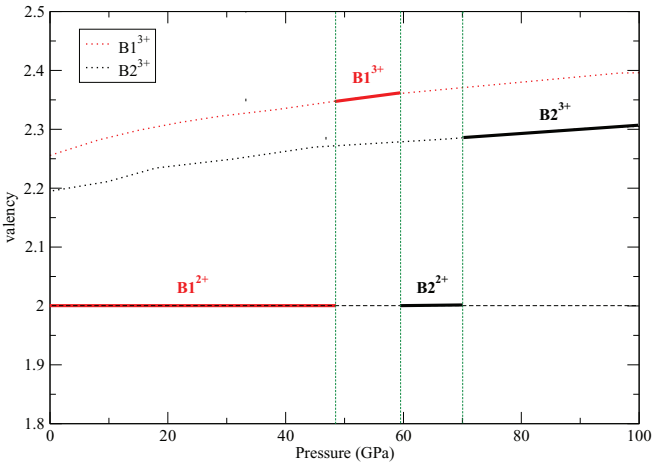

FIG. 6. (Color online) Effective valence of EuO under pressure. Dotted and dashed lines indicate effective valence for the different configurations and structures, solid red and black indicate the actual ground-state valence for the B1 and B2 structures, respectively.

B2 structures, trying to establish how it is influenced by the number of itinerant f electrons and structure. The trivalent $Eu^{3+}(f^6)$ configuration is characterized by six localized f electrons, but the actual number of f electrons is larger, as the occupied f-band states (shown in Fig. 4) also contribute to the total f count on the Eu ion. In Fig. 5 the number of itinerant f electrons in the trivalent configuration for both the B1 and B2 structures is plotted as a function of volume (filled, red and black triangles). We find that for a given volume the number of f electrons n_f is roughly 0.1 electrons higher in the B2 structure compared to the B1 structure. As explained in connection with Figs. 4(a) and 4(b), this difference can be traced to the increased transfer of f electrons to d states due to the increased overlap in the B1 structure. This is confirmed by the number of d electrons, also plotted as a function of volume in Fig. 5 (open, red and black squares), which tends to be roughly 0.1 electrons higher in the B1 structure compared to the B2 structure for any given volume. Going from larger volumes to smaller volumes, the number of f electrons decreases and the number of d electrons increases, showing that the $f \rightarrow d$ transfer is enhanced with pressure. Under pressure the increased overlap between d and f orbitals, on neighboring Eu sites, will lead to further broadening of the d band, and hybridization with the f states, resulting in increased $f \rightarrow d$ transfer.

Under pressure the transition from the Eu^{2+} to the Eu^{3+} configuration occurs once the occupation of the f peak falls below around 0.7 f electrons (indicated by the dashed blue line in Fig. 5). This limit is in line with observations from the earlier SIC-LSD studies on rare earth compounds under external or chemical pressure [35–37]. However, even in the collapsed phase, the fact that the delocalized f electrons are situated in the narrow peak is indicative of heavy fermion behavior, which is not correctly described by LSD. The fractional number of f electrons situated in the peak will still remain largely confined to the Eu sites, and strongly correlated. In this respect, a truly trivalent ground state would imply either a much larger degree of delocalization and hybridization of the f states with the d states, or a complete transfer of $f \rightarrow d$, while the actual valency (which is also the one measured in an experimental study) can be described as intermediate [37], or fluctuating Eu^{3+}/Eu^{2+}, where we associate the number of occupied f-band states n_f with the fraction of Eu^{2+} ions in the system. In the nominal trivalent phase, we can then define an effective valency, equal to $3 - n_f$. For the divalent phase, nominal and effective valences are equivalent. In connection with the evolution of the ground state of EuO, displayed in Fig. 3(a), we can derive the effective valence as a function of pressure from the corresponding number of f-band states. The resulting valency phase diagram is shown in Fig. 6. For pressures below 49 GPa, the seven localized f electrons in the NaCl structure give rise to an effective valency that remains very close to 2+. At the $B1^{2+} \rightarrow B1^{3+}$ transition, the effective valence jumps to ~2.35, and slightly increases under pressure up to around 60 GPa, where the reentrant structural $B1^{3+} \rightarrow B2^{2+}$ results in a drop in the effective valence back to 2+. At 70 GPa the isotructural $B2^{2+} \rightarrow B2^{3+}$ transition results in a valency jumping to 2.3 gradually increasing with further pressure.

According to our calculations, the isostructural $B1^{2+} \rightarrow B1^{3+}$ transition results in an effective valency of roughly 2.35. Instead, Jayaraman *et al.* interpreted the observed volume collapse in terms of a valency change from divalent to trivalent due to $4f \rightarrow 5d$ electron promotion. The idea being that under pressure the gap between conduction band and localized f state gradually closes, and eventually collapses with the resulting f to d transition. The same picture of a closing gap under pressure underlies a number of studies of EuO under pressure, although the views differ as to whether the closure is gradual [12] rather than sudden [11], or whether it results in a hybridization gap [38] rather than a metal-insulator transition [11,12], and finally whether the collapsed phase is intermediate valent rather than integer valent. Zimmer *et al.* [12] estimated that the gradually increasing valency observed in their experiments would reach ~2.5 at pressures of around 35 GPa. In their

electronic structure calculations using a constant U within their LSD+Hubbard 1 scheme, Wan *et al.* [20] attempt to reproduce this evolution in electronic structure under pressure. They find that the gap between f and d states closes at around 10 GPa, but no change in the $4f$ occupation and no sign of valence instability for pressures up to 40 GPa.

The sudden decrease in valency at 60 GPa in Fig. 6, associated with the structural B1→B2 transition is qualitatively rather similar to the one observed in the XANES measurements [15]. However, while our calculations seem to indicate only a narrow pressure region (60 to 70 GPa) with reentrant valence behavior in the CsCl phase, followed above 70 GPa by a trivalent metallic CsCl phase, according to experiment a valence transition from $B2^{2+}\rightarrow B2^{3+}$ is not observed even at 80 GPa. The XANES measurements rely on the EuO and Eu_2O_3 nominal valencies of respectively Eu^{2+} and Eu^{3+}, in order to calibrate their measured valencies. Both reference compounds are insulating, and it is not clear to what degree the Eu L_3 absorption edge in metallic trivalent EuO (i.e., under pressure) is similar to the one observed in insulating trivalent Eu_2O_3. The change in XAS spectra is determined by the core level shifts, which ultimately are determined by the number of localized f electrons, i.e., $Eu^{2+}(f^7)$ in divalent EuO and $Eu^{3+}(f^6)$ in Eu_2O_3 (with a difference in the excitation threshold for the $2p_{3/2} \rightarrow 5d$ transition of ~8 eV [15]). With respect to the total number of (localized + band) f electrons in trivalent EuO, the increase from the B1 to B2 structure would be reflected by a decrease in the excitation threshold as observed in the XAS experiments. Accordingly, even without a full fledged drop in valence to a divalent configuration, the calculated decrease in valence from 2.37 in $B1^{3+}$ below 60 GPa to 2.28 in the $B2^{3+}$ phase above 70 GPa is reminiscent of reentrant behavior, and similar to the drop from 2.2 to 2.05 that is observed experimentally.

IV. SUMMARY AND CONCLUSION

In summary, combining the total energy calculations with experimental pressure data for the structural transitions in EuO under pressure, we have arrived at the following understanding of the sequence of occurring events. Starting from the insulating divalent NaCl phase at ambient pressure, an isostructural insulator to metal transition occurs at around 49 GPa. The resulting $B1^{3+}$ phase is characterized by an effective valency of 2.35. In the pressure range between 49 and 60 GPa, the observed near degeneracy between $B1^{3+}$ and $B2^{2+}$ configurations indicates a possible coexistence of NaCl and CsCl phases with relative proportions that will be highly sensitive to the experimental conditions. At around 60 GPa, a full-fledged structural transition to a reentrant divalent CsCl phase ($B2^{2+}$) occurs, followed at around 70 GPa by a $B2^{2+}\rightarrow B2^{3+}$ valence transition. The occurrence of a divalent CsCl phase between 60 and 70 GPa, as well as the overall decrease in valence from nominally trivalent NaCl phase (effective valence 2.37) to nominally trivalent CsCl phase (effective valence 2.28) are strongly reminiscent of the reentrant valence behavior proposed in the pressure experiments by Souza-Neto *et al.* [15].

ACKNOWLEDGMENTS

This research used resources of the Danish Center for Scientific Computing. This work was supported by EPSRC through a service level agreement with the Scientific Computing Department of STFC. We would like to acknowledge our deceased friend and collaborator Walter Temmerman for his valuable input to the present paper. We believe that his many contributions to the field of strongly correlated d- and f-electron systems will be recognized as his lasting legacy.

[1] L. Petit, R. Tyer, Z. Szotek, W. M. Temmerman, and A. Svane, New J. Phys. **12**, 113041 (2010).
[2] A. Jayaraman, V. Narayanamurti, E. Bucher, and R. G. Maines, Phys. Rev. Lett. **25**, 1430 (1970).
[3] A. Jayaraman, A. K. Singh, A. Chatterjee, and S. U. Devi, Phys. Rev. B **9**, 2513 (1974).
[4] S. Lebègue, G. Santi, A. Svane, O. Bengone, M. I. Katsnelson, A. I. Lichtenstein, and O. Eriksson, Phys. Rev. B **72**, 245102 (2005).
[5] V. Narayanamurti, A. Jayaraman, and E. Bucher, Phys. Rev. B **9**, 2521 (1974).
[6] B. T. Matthias, R. M. Bozorth, and J. H. van Vleck, Phys. Rev. Lett. **7**, 160 (1961).
[7] D. E. Eastman, F. Holtzberg, and S. Methfessel, Phys. Rev. Lett. **23**, 226 (1969).
[8] G. Busch, P. Junod, and P. Wachter, Phys. Lett. **12**, 11 (1964).
[9] J. Schoenes and P. Wachter, Phys. Rev. B **9**, 3097 (1974).
[10] P. G. Steeneken, L. H. Tjeng, I. Elfimov, G. A. Sawatzky, G. Ghiringhelli, N. B. Brookes, and D. J. Huang, Phys. Rev. Lett. **88**, 047201 (2002).
[11] A. Jayaraman, Phys. Rev. Lett. **29**, 1674 (1972).
[12] H. G. Zimmer, K. Takemura, K. Syassen, and K. Fischer, Phys. Rev. B **29**, 2350 (1984).
[13] M. M. Abd-Elmeguid and R. D. Taylor, Phys. Rev. B **42**, 1048 (1990).
[14] S. Heathman, T. LeBihan, S. Darracq, C. Abraham, D. J. A. DeRidder, U. Benedict, K. Mattenberger, and O. Vogt, J. Alloys Compd. **230**, 89 (1995).
[15] N. M. Souza-Neto, J. Zhao, E. E. Alp, G. Shen, S. V. Sinogeikin, G. Lapertot, and D. Haskel, Phys. Rev. Lett. **109**, 026403 (2012).
[16] P. Larson and W. R. L. Lambrecht, J. Phys.: Condens. Matter **18**, 11333 (2006).
[17] S. J. Cho, Phys. Rev. B **1**, 4589 (1970).
[18] M. Betzinger, C. Friedrich, and S. Blügel, Phys. Rev. B **81**, 195117 (2010).
[19] S. Q. Shi, C. Y. Ouyang, Q. Fang, J. Q. Shen, W. H. Tang, and C. R. Li, Eur. Phys. Lett. **83**, 69001 (2008).
[20] X. Wan, J. Dong, and S. Y. Savrasov, Phys. Rev. B **83**, 205201 (2011).

[21] J. M. An, S. V. Barabash, V. Ozolins, M. van Schilfgaarde, and K. D. Belashchenko, Phys. Rev. B **83**, 064105 (2011).
[22] J. Kuneš, W. Ku, and W. E. Pickett, J. Phys. Soc. Jpn. **74**, 1408 (2005).
[23] A. Svane, G. Santi, Z. Szotek, W. M. Temmerman, P. Strange, M. Horne, G. Vaitheeswaran, V. Kanchana, L. Petit, and H. Winter, Phys. Status Solidi b **241**, 3185 (2004).
[24] A. Svane, Phys. Rev. B **53**, 4275 (1996).
[25] W. M. Temmerman, A. Svane, Z. Szotek, H. Winter, and S. V. Beiden, in *Lecture Notes in Physics*, edited by M. Dreyssé (Springer, Berlin, 2000), Vol. 535, p. 286.
[26] J. P. Perdew and A. Zunger, Phys. Rev. B **23**, 5048 (1981).
[27] M. Lüders, A. Ernst, M. Däne, Z. Szotek, A. Svane, D. Ködderitzsch, W. Hergert, B. L. Gyorffy, and W. M. Temmerman, Phys. Rev. B **71**, 205109 (2005).
[28] H. Miyazaki, T. Iti, H. J. Im, K. Terashima, T. Iizuka, S. Yagi, M. Kato, K. Soda, and S. Kimura, J. Phys. Conf. Ser. **200**, 012124 (2010).
[29] O. K. Andersen, Phys. Rev. B **12**, 3060 (1975).
[30] When at pressure P, two phases A and B are at equilibrium, they have the same enthalpy $H(P) = E(P) + PV(P)$, i.e., $H_A(P) = H_B(P)$. The corresponding pressure is derived as $P = -[E_A(P) - E_B(P)]/[V_A(P) - V_B(P)]$, which is the condition for the common tangent.
[31] M. Methfessel, M. van Schilfgaarde, and R. A. Casali, in *Lecture Notes in Physics*, edited by H. Dreysse (Springer, Berlin, 2000), Vol. 535, p. 114.
[32] A. Svane, Solid State Commun. **140**, 364 (2006).
[33] W. M. Temmerman, Z. Szotek, and H. Winter, Phys. Rev. B **47**, 1184 (1993).
[34] A. Svane, N. E. Christensen, L. Petit, Z. Szotek, and W. M. Temmerman, Phys. Rev. B **74**, 165204 (2006).
[35] P. Strange, A. Svane, W. M. Temmerman, Z. Szotek, and H. Winter, Nature (London) **399**, 756 (1999).
[36] L. Petit, A. Svane, Z. Szotek, P. Strange, H. Winter, and W. M. Temmerman, J. Phys.: Condens. Matter **13**, 8697 (2001).
[37] A. Svane, W. M. Temmerman, Z. Szotek, L. Petit, P. Strange, and H. Winter, Phys. Rev. B **62**, 13394 (2000).
[38] D. DiMarzio, M. Croft, N. Sakai, and M. W. Shafer, Phys. Rev. B **35**, 8891 (1987).